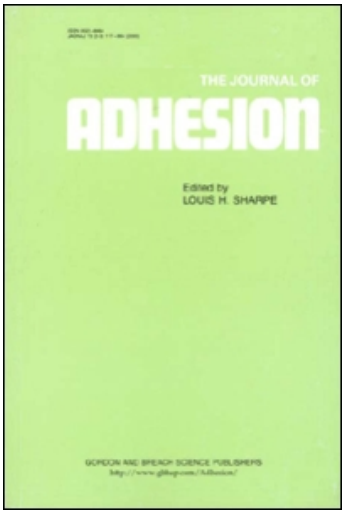


**The Journal of Adhesion**
Publication details, including instructions for authors and subscription information:
http://www.informaworld.com/smpp/title~content=t713453635

# Mode I Fracture Load Predictions of Adhesive T-joints

G. Fernlund[a]; R. Chaaya[a]; J. K. Spelt[a]
[a] Department of Mechanical Engineering, University of Toronto, Toronto, Canada

**To cite this Article** Fernlund, G. , Chaaya, R. and Spelt, J. K.(1995) 'Mode I Fracture Load Predictions of Adhesive T-joints', The Journal of Adhesion, 50: 2, 181 — 190
**To link to this Article: DOI:** 10.1080/00218469508014365
**URL:** http://dx.doi.org/10.1080/00218469508014365

*J. Adhesion*, 1995, Vol. 50, pp. 181–190
Reprints available directly from the publisher
Photocopying permitted by license only



# Mode I Fracture Load Predictions of Adhesive T-joints

G. FERNLUND, R. CHAAYA and J. K. SPELT*

*Department of Mechanical Engineering, University of Toronto, Toronto, Canada M5S 1A4*

*(Received August 29, 1994; in final form January 23, 1995)*

This paper presents fracture data and a finite element analysis for adhesive T-joints, It is shown that fracture loads of T-joints, bonded with two different structural epoxies and subjected to either tensile loading or three-point bending, can be predicted using a fracture mechanics approach. Fracture loads were predicted by calculating the applied energy release rate, $G$, using finite element methods, and comparing that with a critical value, $G_C$, determined experimentally using double-cantilever-beam specimens. By recording the failure sequence of the bondline with a video camera attached to a microscope, it was seen that subcritical crack propagation took place prior to final fracture of the bondline. Accounting for the observed subcritical crack propagation in the finite element analysis gave a good agreement between the actual and the calculated fracture loads.

KEY WORDS: adhesive; T-joint; fracture mechanics; fracture load prediction; finite element analysis



## 1 INTRODUCTION

Adhesive joints can fail in many different ways, but the most critical failure mode is perhaps bondline fracture. Recently, an engineering approach to fracture load predictions of adhesive joints failing by fracture in the bondline was presented.[1,2] It was demonstrated that fracture loads for a wide variety of single-lap-shear, cracked-lap-shear and double-strap joints, with different overlap lengths, adherend thickness and bonded with two different structural epoxies, could be predicted using the approach. The approach is based on fracture mechanics and assumes that the effective loading of the bondline can be described by two parameters: $G$ and $\psi$, where $G$ is the total energy release rate and $\psi = \tan^{-1}(G_{II}/G_I)^{1/2}$ is the phase angle of loading. $G_{II}$ and $G_I$ are the energies released in sliding and opening of the crack, respectively, thus $\psi$ is a measure of the mode mix. Fracture in the bondline is assumed to occur when $G(\psi) = G_C(\psi)$, where $G_C(\psi)$ is the critical energy release rate at the given phase angle (the fracture envelope) and is a measure of the bondline strength. $G_C$ is, in general, dependent on the mode mix, and is typically much lower when the bondline is loaded in opening mode (mode I) than in shearing mode (mode II).[3–5] $G_C(\psi)$ is conveniently determined by fracture tests of adhesively-bonded double-cantilever-beam specimens

* Corresponding author.

subject to mixed mode loading, and has been shown to be independent of adherend geometry for a given adhesive system; *i.e.*, for a given adhesive and adherend material, pretreatment of the adherends, curing time and temperature.[5] Strictly, $G_C(\psi)$ is also dependent on the bondline thickness, but experiments have shown that this dependence is weak for typical bondline thicknesses.[6] For example, double-cantilever-beam specimens bonded with Cybond 4523GB adhesive, with bondline thickness varying from 0.15–1.2 mm, were subject to mode $I(\psi = 0°)$ and mixed mode loading ($\psi = 41°$). No significant difference in $G_C$ was observed, based on 66 and 41 crack extension events in mode I and mixed mode, respectively.[6] Similar results for this type of adhesive have been reported earlier.[7,8]

Once $G_C(\psi)$ has been determined experimentally for an adhesive system, failure loads for joints of any geometry using this adhesive system can be predicted by calculating the applied $G$ and $\psi$. Fracture load predictions reduce to the calculation of $G$ and $\psi$ for the considered joint configuration, and comparison with the experimentally-determined $G_C(\psi)$. The approach allows the fracture load to be predicted for both cracked and uncracked joints. By video taping the failure sequence of uncracked epoxy joints, it was seen that the adhesive spew fillet broke at a load significantly lower than the ultimate fracture load, and that breaking of the fillet did not cause final separation of the adherends.[9] When the load was increased after the fillet broke, subcritical crack propagation was observed in the bondline until the applied load reached a maximum value and final fracture occurred. Hence, final fracture was seen to occur from a cracked bondline, which makes the present fracture mechanics approach for the prediction of the ultimate fracture load applicable even to initially-uncracked joints.

The observed subcritical crack propagation under increasing applied load occurred because the tested adhesives exhibited a rising $R$-curve behaviour that increased the *in-situ* fracture toughness of the bondline as the crack grew, until steady-state conditions were obtained.[5] The amount of subcritical crack propagation required to obtain steady-state conditions ($G_C$ independent of the crack length) is dependent on the adhesive system and the mode of loading.[9]

In a previous paper, the applied energy release rate, $G$ and the mode mix, $\psi$, for single-lap-shear, cracked-lap-shear and double-strap joints were calculated using an analytical technique based on beam theory to enable fracture load predictions.[1] This technique is applicable to a large class of lap-strap joints, but is not applicable to joints with more complex shapes. For joints with more complex shapes, analytical closed-form solutions are unavailable. The objective of the present study was to determine whether fracture loads for joints with more complex shapes can be predicted using a numerical technique to calculate $G$ and $\psi$. In this paper, fracture loads of adhesively-bonded T-joints are predicted by calculating $G$ and $\psi$ using finite element analysis and comparing with an experimentally-determined value of $G_C$ as described above for planar joints. The T-joints were subjected to tensile loading and three-point-bending, both resulting in mode I loading of the bondline (Fig. 1). No mixed-mode conditions were tested due to the difficulties in devising an appropriate test specimen. It is shown that subcritical crack propagation and the rising R-curve behaviour of the adhesive are important for fracture load predictions. T-joints represent a class of joints which might include bonded brackets and extrusion profiles, in which the fracture is dominated by tensile stresses.

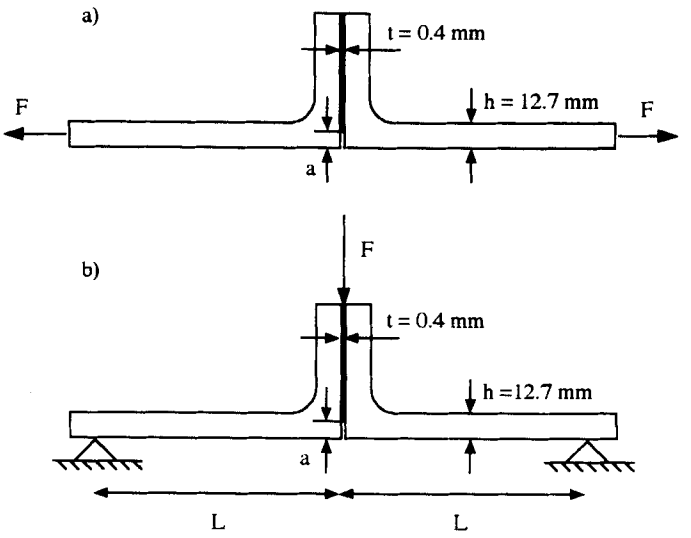


FIGURE 1 T-joints subjected to tensile loading (a) and three-point bending (b).



## 2 EXPERIMENTS

Adhesively-bonded T-joints subjected to tensile loading and three-point bending were loaded to failure. The joints were manufactured in batches by bonding 6061-T6 aluminum alloy angles of height $h = 12.70$ mm back-to-back (Fig. 1). The angles were acetone degreased, immersed in industrial detergent (P3 Almecho), and pretreated using an FPL-etch (ASTM D2651-79, method G). An even bondline of 0.4 mm thickness was obtained using Teflon spacers, and the joints were cured at 150°C for 150 minutes. Specimens were bonded using two different single-part structural epoxies: the mineral-filled Cybond 4523 GB (American Cyanamid) and the rubber-toughened ESP 310 (Permabond). The Cybond 4523 GB has a Young's modulus of 8 GPa,[11] whereas the ESP 310 is less stiff and significantly tougher. After curing, the batches were cut into test specimens with a width of 20 mm.

The bondlines were either left intact or were given a starter crack of length $a = 6.35$ mm or $a = 12.7$ mm using a fine saw (Fig. 1). In total, thirty-four specimens were tested to failure. Twelve specimens bonded with the ESP 310 adhesive were subjected to tensile loading: four with no precrack, four with a 6.35 mm starter crack, and four with a starter crack of 12.7 mm. Six specimens bonded with the ESP 310 adhesive were subjected to three-point bending: two with no precrack, two with a 6.35 mm starter crack, and two with a starter crack of 12.70 mm. A similar test series was performed with specimens bonded with the Cybond 4523GB adhesive, with the difference that no three-point bend specimens with an initial crack length of 12.70 mm were tested. The tests were performed under displacement control and with a cross-head speed of 2 mm/min. As expected, joints without initial starter cracks failed at much higher loads than joints with starter cracks.

The bondline behaviour during the experiments was recorded with a video camera attached to a microscope. By studying the recorded failure sequence frame by frame after the test had been performed, it was seen that subcritical crack propagation occurred in the bondline prior to final fast fracture. The subcritical crack propagation was virtually impossible to detect without the use of a video camera because it happened during the last few seconds before final fast fracture, and the extent of the subcritical crack growth was approximately 2–4 mm (one bondline thickness = 0.4 mm), independent of initial crack length. For the ESP 310 adhesive, the length of the subcritical crack growth could also be measured on the fracture surface after the test. The fracture surface corresponding to the slower subcritical crack propagation was visibly different from the fracture surface corresponding to fast final fracture for the ESP 310 adhesive, whereas no distinguishing features were observed for the Cybond 4523GB adhesive.

## 3 ANALYSIS

By subjecting the T-joints to tensile loading and three-point bending, the crack in the bondline is subject to mode I or opening mode (Fig. 1). The average *in-situ* critical energy release rates in mode I, $G_{IC}$, for the two tested adhesive systems were determined with double-cantilever-beam specimens to be 270 J/m$^2$ and 1150 J/m$^2$, for specimens bonded with Cybond 4523GB and ESP 310, respectively. Note that these values are somewhat higher than previously-published data for these adhesive systems, due to batch-to-batch variation in the adhesives received from the manufacturers.[5]

To predict the fracture loads for the two different loading configurations, the energy release rate, $G$, was calculated and compared with the experimentally-determined values of $G_{IC}$ presented above. Because of the complex shape of the T-joint, finite element analysis was used to calculate $G$ for different crack lengths.

The energy release rate, $G$, of a cracked linear elastic body is, in general, dependent on the geometry of the body and the Young's modulus, and is proportional to the applied load squared. Conservation of the J-integral gives that, for the purpose of calculating $G$, an adhesively-bonded specimen with a thin adhesive layer can be treated as being homogeneous (consisting entirely of adherend material) provided that the crack length is much larger than the thickness of the adhesive layer.[10] In the present case, the thickness of the adhesive layer ($t = 0.4$ mm) is much less than the angle height ($h = 12.70$ mm). The stiffness of the adhesive layer is much less than the stiffness of the adherends (8 Gpa *vs* 70 GPa for the Cybond 4523GB, and less for the ESP 310); furthermore, the considered crack lengths are at least 2 mm, which justifies the neglect of the adhesive layer in the calculations.

For a T-joint subjected to a tensile load, $F$, the geometry is characterized by the crack length, $a$, and the angle height, $h$ (Figure 1a). The length of the bonded overlap and the sections where the load is applied are long enough so as not to enter into the problem. Hence, for the T-joint shown in Figure 1a

$$G = F^2 f(E, a, h) \tag{1}$$

where $F$ is the applied load per unit width, $E$ is the Young's modulus of the angles and $f(E, a, h)$ is some undetermined function. Dimensional considerations give that Equation (1) can be written

$$G = \frac{F^2}{Eh}\phi_T(a/h) \tag{2}$$

where $\phi_T(a/h)$ is a dimensionless function that uniquely characterizes the dependence on the crack length, $a$.[11] To determine $\phi_T(a/h)$, a series of finite element calculations with different crack lengths were performed using the ANSYS (version 4.4a) finite element package. The T-joint shown in Figure 1a was treated as being homogeneous, neglecting the adhesive layer, and was modeled using plane stress, six-noded, quadratic isoparametric triangular elements; measurements with strain gauges have shown that the adherends are approximately under plane stress when the adherends have a height-to-width ratio of 12.7 mm/20 mm, as in the present case.[12] A fine mesh, with singular elements in the region close to the crack tip, was obtained using the KSCON utility in the ANSYS package. The stress intensity factor, $K_I$, was calculated from the displacement field behind the crack tip using a built-in routine. Using $G = (K_I)^2/E$, and assuming plane stress conditions, the dimensionless function could be calculated from $\phi_T(a/h) = h(K_I/F)$.[2] The calculated values of $\phi_T(a/h)$ are listed in Table I. A non-linear regression curve-fit to these data gives

$$\phi_T(a/h) \approx 8.28(a/h)^3 - 0.89(a/h)^2 + 5.65(a/h) + 0.03 \tag{3}$$

For a T-joint subjected to three-point bending, the geometry is characterized by the crack length, $a$, the angle height, $h$, and the distance between the support and the crack tip, $L$(Figure 1b). Following the reasoning above, the energy release rate for the T-joint shown in Figure 1b can be expressed as

$$G = F^2 f(E, a, h, L) \tag{4}$$

where $F$ is the applied load per unit width, $E$ is the Young's modulus of the angles, and $f(E, a, h, L)$ is some undetermined function. Dimensional considerations give that Equation (4) can be written

$$G = \frac{F^2}{Eh}\phi_B(a/h, L/h) \tag{5}$$

TABLE I
Geometry function, $\phi_T(a/h)$, for tensile loaded T-joints

| $a/h$ | $\phi_T(a/h)$ |
|---|---|
| 0.10 | 0.59 |
| 0.25 | 1.51 |
| 0.50 | 3.66 |
| 0.75 | 7.26 |
| 0.90 | 10.43 |

where $\phi_B(a/h, L/h)$ is a dimensionless function that uniquely characterizes the dependence on the crack length and the distance between the support and the crack tip. In the present case, $L/h$ was held constant and the only variable was $a/h$. To determine $\phi_B(a/h, L/h)$ in Equation (5), another series of finite element calculations with various crack lengths, $a$, were performed using the ANSYS finite element package as described above. The calculated values of $\phi_B(a/h, L/h)$ with $L/h = 8.91$ are presented in Table II. A non-linear regression curve-fit to the data in Table II gives

$$\phi_B(a/h) \approx 2.52(a/h)^3 - 28.62(a/h)^2 + 192.07(a/h) + 1.72 \quad (6)$$

With the two geometry functions $\phi_T(a/h)$ and $\phi_B(a/h)$ determined, the energy release rates for the tensile-loaded and three-point bend loaded T-joints can be calculated for any crack length ($0.1 < a/h < 1$) using Equations (2) and (5).

## 4 COMPARISON OF ACTUAL AND PREDICTED FRACTURE LOADS

The $G_{IC}$ values for the two adhesives presented above, 270 J/m$^2$ (Cybond 4523 GB) and 1150 J/m$^2$ (ESP 310), are the values corresponding to steady-state conditions or the plateau value of the R-curve. Fracture toughness data are sometimes determined with specimens having a sharp starter crack (giving values corresponding to the beginning of the R-curve), but the steady-state values are of more interest for the prediction of the ultimate fracture load of an adhesive joint. Ultimate fracture loads (max. load after subcritical crack growth) for tensile-loaded and three-point bend loaded T-joints can be calculated by equating the analytical expression for $G$, Equation (2) or (5), to $G_{IC}$ for the given adhesive system and solving for the applied force, $F$. For the technique to give good results, the observed subcritical crack propagation must be accounted for when calculating $G$, since the above $G_{IC}$ values are the steady-state values. Thus, the crack length, $a$, in Equations (2) and (5) should be the initial crack length, $a_0$, plus the observed subcritical crack propagation prior to final fracture, $\Delta a$.

Twelve specimens bonded with the ESP 310 adhesive where subjected to tensile loading (Fig. 1a): four with no starter crack, four with a 6.35 mm starter crack, and four with a 12.70 mm starter crack. Estimates from the video tape and measurements on the fracture surface showed that the amount of subcritical crack propagation, $\Delta a$, was between 2 mm and 4 mm with an average of 2.8 mm prior to final fracture. The average values of the recorded ultimate fracture loads per unit width at each initial crack length

TABLE II
Geometry function, $\phi_B(a/h, L/h)$, for T-joints in three-point bending

| $a/h$ | $\phi_B(a/h, L/h)$ ($L/h = 8.91$) |
|---|---|
| 0.10 | 20.58 |
| 0.25 | 48.13 |
| 0.50 | 90.74 |
| 0.75 | 130.88 |
| 0.90 | 153.18 |

are shown in Figure 2 together with the predicted fracture loads assuming 2 and 4 mm of subcritical crack propagation, respectively. The standard deviation of the data was so small that the error bars are within the square symbols of Figure 2. As seen from Figure 2, basing the calculations on $\Delta a = 2$ mm leads to an overestimate of the ultimate fracture load, and basing them on $\Delta a = 4$ mm leads to an underestimate. If the measured average of $\Delta a$ is used ($\Delta a = 2.8$ mm), the agreement between the predicted and actual fracture loads is very good.

Figure 3 shows a comparison of the actual and predicted ultimate fracture loads per unit width for T-joints bonded with the Cybond 4523 GB adhesive and subjected to tensile loading. Four specimens were tested at each of the initial crack lengths and the average values of the fracture loads per unit width are presented in Figure 3. The standard deviation was so small that the error bars can only be seen for $a_0 = 0$. The amount of subcritical crack propagation could not be measured from the fracture surface for this adhesive. However, the video tape showed that the amount of subcritical extension was approximately the same for both adhesive systems, so the values of $\Delta a = 2$ mm and $\Delta a = 4$ mm were again used as lower and upper limits. If $\Delta a = 2$ mm is used in the calculations, the fracture loads are overestimated, whereas if $\Delta a = 4$ mm is used, the fracture loads are underestimated. Comparison of Figures 2 and 3 reveals that the ultimate fracture loads for specimens bonded with ESP 310 are approximately twice those for specimens bonded with Cybond 4523 GB. This was expected because $G$ is proportional to the applied load squared, and $G_{IC}$ is approximately four times higher for ESP 310 than for Cybond 4523GB.

A smaller series of fracture tests with T-joints subjected to three-point bending was performed (six specimens bonded with ESP 310 and four specimens bonded with



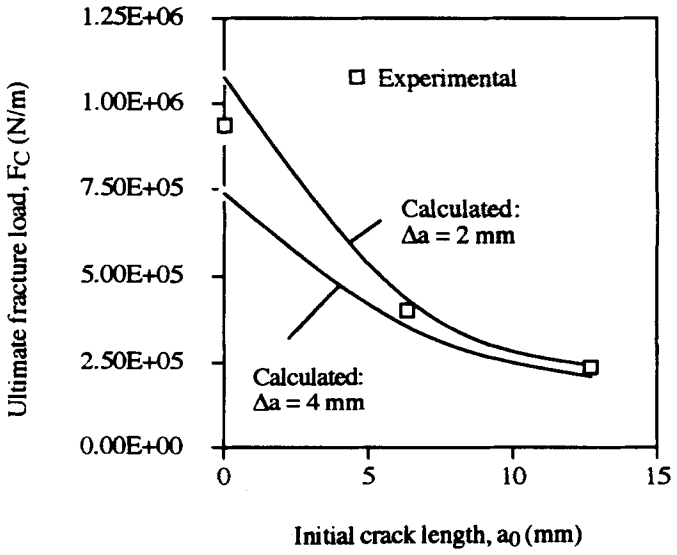


FIGURE 2 Comparison of experimental and calculated ultimate fracture loads per unit width for T-joints bonded with ESP 310, subjected to tensile loading (Fig. 1a).

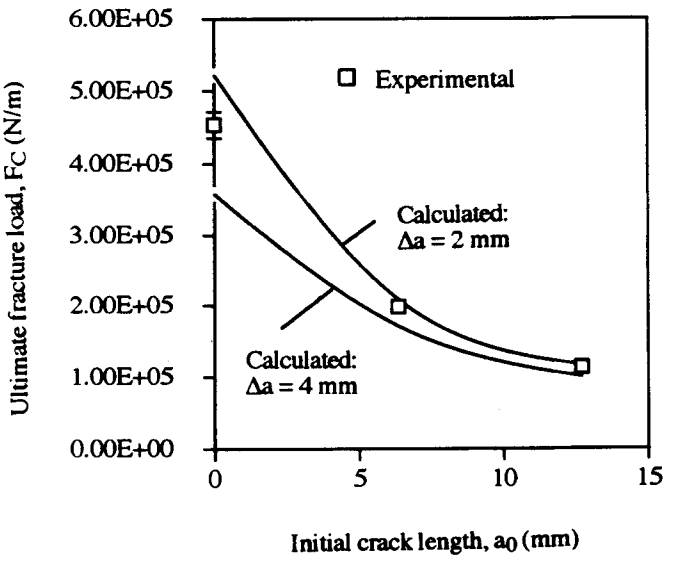


FIGURE 3 Comparison of experimental and calculated ultimate fracture loads per unit width for T-joints bonded with Cybond 4523 GB, subjected to tensile loading (Fig. 1a).



Cybond 4523 GB) to see if the good agreement between predicted and actual fracture loads could be repeated for a different type of loading. Figures 4 and 5 show comparisons between actual and predicted ultimate fracture loads per unit width for T-joints, bonded with ESP 310 and Cybond 4523 GB respectively, subject to three-

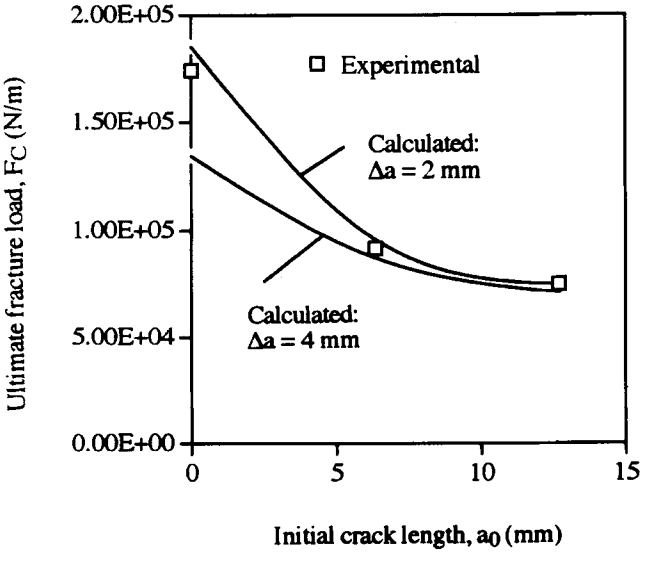


FIGURE 4 Comparison of experimental and calculated ultimate fracture loads per unit width for T-joints bonded with ESP 310, subjected to three-point bending (Fig. 1b).

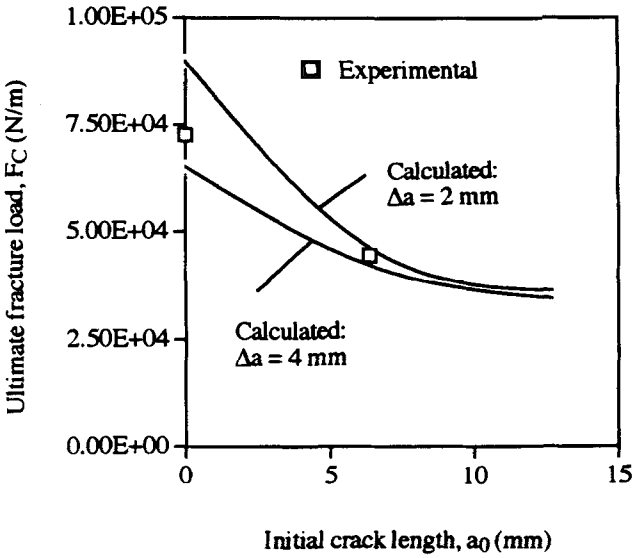


FIGURE 5 Comparison of experimental and calculated ultimate fracture loads per unit width for T-joints bonded with Cybond 4523 GB, subjected to three-point bending (Fig. 1b).



point bending. The data scatter was again so small that the error bars are within the square symbols of Figures 4 and 5. By video taping the bondline during the test, it was seen that the amount of subcritical crack propagation, $\Delta a$, was approximately 2–4 mm, as before. $\Delta a$ could not be measured from the fracture surface for either adhesive because ultimate fracture occurred in a slower, more stable, manner than for the case of tensile loading. Again, it is seen that $\Delta a = 2$ mm leads to an overestimate of the predicted fracture loads and that $\Delta a = 4$ mm leads to an underestimate. Note that only two specimens were tested at each crack length in this case, and that no specimen bonded with the Cybond 4523 GB adhesive was tested with an initial crack length of 12.70 mm.

## 5 DISCUSSION AND CONCLUSIONS

If the subcritical crack propagation is omitted in the calculation of $G$, the predicted ultimate fracture loads will be significantly higher than the actual ones because the $G_{IC}$ values were determined at steady-state crack conditions. Figures 2 to 5 show that a good agreement between the actual and predicted fracture loads is obtained in all cases if the measured average subcritical crack propagation prior to ultimate fracture, $\Delta a = 2.8$ mm, is added to the initial crack length, $a_0$, in the calculation of $G$. Figures 2 to 5 also show that the predicted fracture loads are sensitive to the choice of $\Delta a$ (a parameter that is difficult to measure and determine accurately), if the initial crack length is relatively small. However, if the maximum measured value, $\Delta a = 4$ mm, is used in the calculations of $G$, a conservative estimate of the actual fracture load is obtained.

The experiments showed that the amount of subcritical crack growth that occurred prior to final fracture, $\Delta a$, was independent of the initial crack length and was approximately the same for the two tested adhesive systems. Previous tests have shown that $\Delta a$ is dependent on the mode of loading with $\Delta a \approx 5$–$7$ mm when $\psi \approx 65°$ and $\Delta a \approx 10$ mm when $\psi \approx 90°$ (model II).[9] This dependence of $\Delta a$ on mode mix must be accounted for if accurate predictions of the ultimate fracture load are to be made for joint geometries in which $G$ is strongly dependent on the crack length. Because $\Delta a$ was seen to be approximately the same for the two tested epoxy adhesives (one mineral-filled and one rubber-toughened), the present values of $\Delta a$ may serve as an initial estimate for the purpose of engineering calculations with structural epoxies.

## Acknowledgement

The authors are grateful for the support of American Cyanamid, the Natural Sciences and Engineering Research Council of Canada, and the Manufacturing Research Corporation of Ontario.

## References

1. G. Fernlund, M. Papini, D. McCammond and J. K. Spelt, *Comp. Sci. & Tech.* **51,** 587 (1994).
2. M. Papini, G. Fernlund and J. K. Spelt, *Int. J. Adhesion and Adhesives* **14,** 5 (1994).
3. K. M. Liechti and T. Freda, "Advances in Adhesively Bonded Joints", *ASME Winter Annual Meeting*, Chicago, III., p. 65 (1988).
4. P. Davies *et al.*, *Comp. Sci. & Tech.* **43,** 129 (1992).
5. G. Fernlund and J. K. Spelt, *Comp. Sci. & Tech.*, **50,** 441 (1994).
6. E. K. Y. Wong, B. A. Sc. thesis, Dept. of Mech. Eng., University of Toronto (1994).
7. H. Chai, *Int. J. Fracture* **37,** 137 (1988).
8. G. Fernlund, and J. K. Spelt, *Int. J. Adhesion and Adhesives* **11,** 221 (1991).
9. M. Papini, G. Fernlund and J. K. Spelt, *Comp. Sci & Tech.* **52,** 561 (1994).
10. J. W. Hutchinson and Z. Suo, *Adv. in Appl. Mech.* **29,** 172 (1992).
11. G. Fernlund and J. K. Spelt, *J. Comp. Tech. & Res.* **16,** 234 (1994).
12. D. Plausinis, M. A. Sc. thesis, Dept. of Mech. Eng. University of Toronto (1994).